Disruption of *Escherichia coli* transaldolase into catalytically active monomers: evidence against half-of-the-sites mechanism

Ulrich Schörken[a], Jia Jia[b], Hermann Sahm[a], Georg A. Sprenger[a], Gunter Schneider[b,*]

[a] *Institut für Biotechnologie 1, Forschungszentrum Jülich GmbH, P.O. Box 1913, D-52425 Jülich, Germany*
[b] *Division of Molecular Structural Biology, Department of Medical Biochemistry and Biophysics, Karolinska Institutet, Doktorsringen 9, S-171 77 Stockholm, Sweden*

Received 13 October 1998

Abstract Disruption of the hydrogen bonding network at the interface of *Escherichia coli* transaldolase by substitution of R300 to a glutamic acid residue resulted in a monomeric enzyme at basic pH values, with almost no change in the kinetic parameters. The stability of the R300A and R300E mutants towards urea and thermal inactivation is similar to that of the wild-type enzyme. X-ray analysis showed that no structural changes occurred as a consequence of the side chain replacement. This indicates that the quaternary structure is not required for catalytic activity nor does it contribute significantly to the stability of the enzyme. The results are not consistent with a proposed half-of-the-sites reaction mechanism.

Key words: Class I aldolase; Transaldolase; Site-directed mutagenesis; Protein crystallography; Half-of-the-sites mechanism

1. Introduction

Aldolases have been classified into two families, class I and class II, based on their reaction mechanism [1,2]. The class I aldolases catalyze chemical reactions using an active-site lysine residue to form a Schiff-base intermediate with their substrates. The ubiquitous enzyme transaldolase (EC 2.2.1.2) belongs to the class I aldolase family, and it catalyzes the reversible transfer of a dihydroxyacetone moiety, derived from fructose 6-phosphate to erythrose 4-phosphate yielding sedoheptulose 7-phosphate and glyceraldehyde 3-phosphate [3]. The three-dimensional structure of transaldolase B from *Escherichia coli* consists of one domain, folded into an α/β barrel [4]. A comparison of the structure of transaldolase with that of fructose 1,6-bisphosphate aldolase led to the conclusion that transaldolase most probably has arisen as a result of a circular permutation of an ancestral class I aldolase gene [4,5].

Transaldolase from *E. coli* is a homodimer, and the distance between the two active sites is approximately 45 Å. One important subunit-subunit interaction is a hydrogen bond from the side chain of R300 to the main chain oxygen atom of N286. This arginine residue is also involved in charge compensation of the side chains of D293 and E297 at this interface region. In order to address the question whether the quaternary structure is necessary for catalytic activity, we disrupted this network of hydrogen bonds and charge interactions by site-directed mutagenesis with the aim of producing monomeric transaldolase. In this communication, we report the consequences of the replacement of the invariant residue R300 by alanine and glutamic acid for the kinetic and structural properties of the mutant enzymes. Our results do not favor a half-of-the-sites mechanism which had been proposed for the yeast enzyme [6].

2. Materials and methods

2.1. Chemicals

Sugar phosphates and urea were purchased from Sigma, Deisenhofen, Germany. The auxiliary enzymes triosephosphate isomerase/glycerol 3-phosphate dehydrogenase, and restriction enzymes were obtained from Boehringer, Mannheim, Germany. Oligonucleotides for sequencing, mutagenesis, and selection were custom-synthesized. The 'plasmid Mini' DNA preparation kit was obtained from Qiagen, Hilden, Germany and the 'Chameleon' double-stranded mutagenesis kit was supplied by Stratagene, La Jolla, CA, USA. Q-Sepharose HP, fluorescent-labelled ATP and the 'Auto Read' sequencing kit was purchased from Pharmacia, Freiburg, Germany and DEAE 650 M from Merck, Darmstadt, Germany. Glycylglycine and NADH were obtained from Biomol, Hamburg, Germany and all microbiological media were supplied by Difco.

2.2. Site-directed mutagenesis

Site-directed mutagenesis of the talB gene was performed with a modified version of the method of Deng and Nickoloff [7] on the talB-encoding plasmid pGSJ451 [8] using the 'Chameleon' kit (Stratagene, San Diego, CA, USA). The selection primer was 5′ CTG TGA CTG GTG ACG CGT CAA CCA AGT C 3′, and the respective mutagenesis primers were R300A: 5′ CTG GCG GAA GGT ATC GCG AAG TTT GCT ATT GAC 3′ and R300E: 5′ CTG GCG GAA GGT ATC GAA AAG TTT GCT ATT GAC 3′. Plasmid DNA which had not annealed with the selection primer was restricted with Asp-700. DNA was transformed into *E. coli* XLmutS, reisolated and digested with Asp-700 again before transforming *E. coli* DH5 cells. Clones were analyzed by DNA sequencing using the non-radioactive fluorescent technique in conjunction with the automated ALF sequencer and the protocol of the supplier (Pharmacia).

2.3. Enzyme purification and activity measurements

Transaldolase variants were purified to homogeneity according to the purification scheme of the wild-type enzyme [8]. For all activity measurements the formation of glyceraldehyde 3-phosphate from fructose 6-phosphate was monitored by the decrease of NADH at 340 nm as described before [3,8]. The K_M values for fructose 6-phosphate (concentration interval 0.05–100 mM) were determined at a constant concentration of 1.5 mM erythrose 4-phosphate, while the K_M for erythrose 4-phosphate (concentration interval 50 μM–5 mM) was determined at a constant cosubstrate concentration of 50 mM fructose 6-phosphate. All measurements were carried out in duplicate. K_M and V_{max} values were calculated with the program Origin according to first-order Michaelis-Menten kinetics.

2.4. Urealthermal inactivation

For the inactivation experiments, enzyme concentrations were adjusted to 1 mg/ml. The protein concentrations were estimated by a dye-binding method [9]. The enzymes were incubated in 50 mM glycylglycine, pH 8.5 containing 1 mM dithiothreitol at different temperatures up to 55°C for 40 min and at room temperature with varying urea concentrations (up to 5 M) for 150 min. Prior to activity meas-

*Corresponding author.

PII: S0014-5793(98)01521-X

urements, enzymes were diluted so that the final temperature was 30°C and the final urea concentration was below 50 mM for all samples.

2.5. Crystallography

Enzyme samples were concentrated to about 20 mg/ml. Crystals of transaldolase mutants were obtained using the same protocol as for the wild-type enzyme [10], with 11–13% (w/w) PEG-6000 in 0.1 M sodium citrate buffer at pH 4.0. Microseeds from wild-type transaldolase were used for microseeding. Crystals of R300A were isomorphous to the crystals of the wild-type enzyme (form A) described previously [10], space group $P2_12_12_1$, with cell dimensions $a = 69.2$ Å, $b = 92.0$ Å and $c = 130.5$ Å. R300E crystallized in space group $P2_12_12_1$, with cell dimensions $a = 68.9$ Å, $b = 87.7$ Å and $c = 131.5$ Å (form B). All diffraction data sets were collected on a MAR Research imaging plate mounted on a Rigaku rotating anode at 293 K. Data processing and scaling was carried out using DENZO and SCALEPACK [11] and details of the data collection are given in Table 1. The structures of the transaldolase mutants were solved by difference Fourier methods. Initial phases for mutant R300A were calculated from the coordinates of the wild-type enzyme [4]. Phases for mutant R300E were obtained from a model of the native enzyme in crystal form B, obtained by molecular replacement and refined to *R*-free of 26.9% at 2.2 Å resolution [12]. Model building was carried out with the program O [13]. The protein models were refined with X-PLOR [14], using the parameters described by Engh and Huber [15]. The crystal asymmetric unit contains two subunits related by a translation and tight non-crystallographic symmetry restraints were kept throughout the refinement. All protein models were analyzed with PROCHECK [16]. Details of the refinement statistics are given in Table 1.

3. Results

3.1. Kinetic properties of mutant transaldolase

The kinetic parameters of wild-type and mutant transaldolases R300A and R300E are summarized in Table 2. The catalytic activities of mutant enzymes were not severely impaired by the amino acid substitutions. The specific catalytic activities of R300A and R300E were close to that of the wild-type enzyme, 76.4% and 84.1%, respectively. The K_M values for the substrates fructose 6-phosphate and erythrose 4-phosphate were also very little affected.

Table 1
Statistics of data collection and refinement

	R300A	R300E
Data collection:		
Resolution (Å)	2.10	2.20
Highest resolution shell	2.15–2.10	2.25–2.2
Measured reflections	281 960	179 971
Unique reflections	43 810	34 779
Completeness (%)	88.5	84.4
Highest resolution shell (%)	73.7	76.0
I/σ	7.3	7.5
Highest resolution shell	1.8	1.8
R-merge (%)	5.4	6.8
Highest resolution shell (%)	36.4	32.4
Refinement:		
Resolution interval (Å)	10–2.10	10–2.20
R-factor (%)	20.1	20.2
R-free (%)[a]	24.7	25.0
Non-hydrogen atoms of protein	4928	4936
Water molecules	483	406
Average B factors (Å^2)		
Protein atoms	24.90	26.93
Solvent atoms	41.11	37.33
rms bond length deviation (Å)	0.007	0.006
rms bond angle deviation (°)	1.5	1.5
rms B factor (Å^2)	1.7	1.6
Ramachandran plot: % of residues		
in the most favorable region	96.3	95.5
in disallowed regions	0.0	0.0

[a]Calculated on 5% of the reflections not included in the refinement.

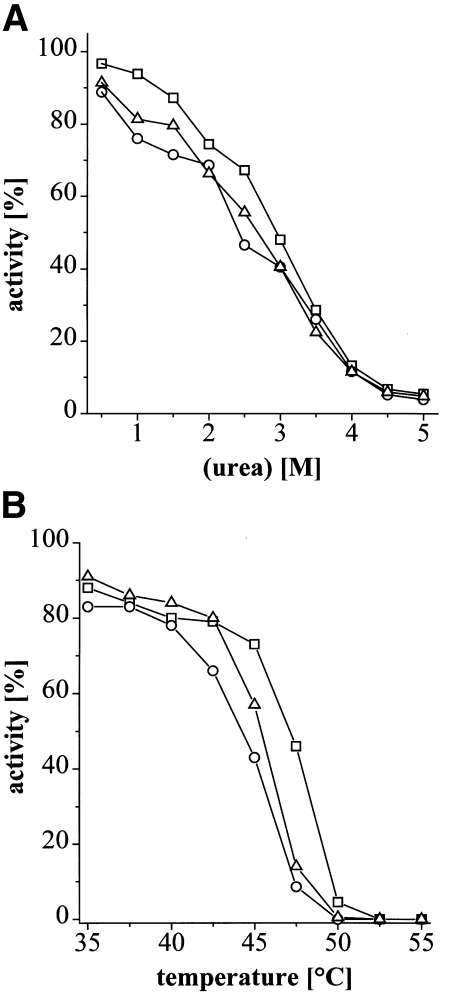

Fig. 1. Effect of quaternary structure on the stability of transaldolase. Wild-type enzyme (squares), R300A (circles) and R300E (triangles) were incubated in 50 mM glycylglycine, pH 8.5, 1 mM DTT for 150 min in varying concentrations of urea (A) and for 40 min at varying temperatures (B).

3.2. Quaternary structure and stability of mutant transaldolase

The determination of the molecular mass of the transaldolase mutants at position 300 was carried out by gel filtration chromatography (Table 3). At pH 8.5 (which is close to the pH optimum of the wild-type enzyme [8]) the calculated molecular mass of the R300E mutant is consistent with a monomeric structure, whereas the molecular mass for the R300A mutant (49 kDa) is inconclusive. This value is about halfway between the molecular mass of a monomer (35 kDa) and dimer (70 kDa) and might represent a fast equilibrium between monomers and dimers for this particular mutant. At pH 4.5, both mutants give molecular masses similar to the wild-type enzyme, indicating that at low pH they form a dimer. This is consistent with the crystal structure, determined at pH 4.0, which shows dimer formation in the crystal for R300A and R300E in a similar manner to wild-type transaldolase (see below). Substitutions of R300 resulted in very minor changes in stability of the mutant enzymes towards urea or thermal inactivation (Fig. 1). A decrease in stability

Table 2
Kinetic parameters for wild-type and mutant transaldolase

Enzyme	V_{max} [μmol/min/mg]	% V_{max}	K_M [μM]	% K_M	k_{cat}/K_M [1/M/s]	% k_{cat}/K_M	K_M [μM]	% K_M	k_{cat}/K_M [1/M/s]	% k_{cat}/K_M
			fructose 6-phosphate				Erythrose 4-phosphate			
Wild-type	54.9		940		69 000		295		244 000	
R300A	40.8	74.3	1350	144	37 500	54.3	265	90	205 000	86.1
R300E	42.8	78.0	1200	128	40 200	58.3	350	119	174 000	73.1

Table 3
Quaternary structure of transaldolase mutants

Protein	pH 4.5			pH 8.5		
	Vel (ml)	M_r	Structure	Vel (ml)	M_r	Structure
Wild-type	73.82	70 000 ± 10 000	dimer	72.17	70 000 ± 10 000	dimer
R300A	74.41	67 000 ± 10 000	dimer	76.95	49 000 ± 8 000	monomer/dimer
R300E	74.67	65 000 ± 10 000	dimer	81.46	33 000 ± 5 000	monomer

towards thermal inactivation can be seen in particular for the R300A mutant, whereas the changes in stability towards urea are probably not significant.

3.3. Crystal structures of transaldolase mutants

The mutant enzymes R300A and R300E were crystallized isomorphously to the wild-type enzyme. The crystal structures were determined using difference Fourier methods and refined at 2.05 and 2.2 Å resolution, respectively. The electron density for the polypeptide chains and amino acid side chains is well defined in both mutants and the electron density maps clearly show the side chain replacement in each of the mutants. The overall structures of the mutant transaldolases are similar to that of the wild-type enzyme and no large conformational changes were found as a consequence of the side chain replacement. The overall rms deviations for 316 Cα atoms between the wild-type enzyme and the mutants are 0.16 Å (R300A), and 0.29 Å (R300E), respectively. The largest structural differences were found in mutant R300E, where a loop region between helices αD and α6 is shifted by about 1 Å from its position in the structure of the wild-type enzyme. This structural change is due to differences in crystal packing rather than amino acid substitution. The R300E mutant crystallized in a crystal form (form B) different from the form A crystals described by Jia et al. [10]. In this new crystal form, the tight crystal packing causes a movement of the exposed loop αD–α6 closer to the enzyme surface, resulting in a tighter interaction. Wild-type transaldolase can also give form B crystals and a similar structural change has been observed [12]. The R300A and R300E transaldolases form dimers in the crystal lattice in the same manner as the wild-type enzyme. A closer inspection of the interface regions in the two mutants reveals only very small adjustments of side chains in the vicinity of the mutagenesis site that are required to accommodate the amino acid substitution. The largest side chain movement is observed in the R300E mutant. The side chain of E300 points into a direction different from the arginine side chain in the wild-type enzyme and forms a hydrogen bond with the side chain of Q287 from the second subunit. In turn, this side chain moved about 2.4 Å towards the enzyme surface from its position in the wild-type enzyme to avoid too close contacts with the side chain of E300 (Fig. 2).

4. Discussion

Replacement of the conserved residue R300 at the subunit-subunit interface by alanine or glutamic acid prevents formation of stable dimers at high pH. This observation is consistent with the crystal structure, which shows that this residue is part of a network of hydrogen bonds and charges (Fig. 2). Both substitutions resulted in a surplus of negative charges at this part of the interface, thus severely impairing dimer formation. The substitution R300E had, in agreement with our expectations, a more damaging effect on quaternary structure than the substitution by alanine, since it introduces an additional negative charge close to D293 and E297. The fact that at low pH dimers can be formed supports the notion of charge repulsion as a primary cause of the observed changes in quaternary structure. At pH 4.0, the glutamic and aspartic acid side chains will be protonated to a substantial extent and the dimeric quaternary structure can be maintained. Mutants at position 300 retained more than 75% of the catalytic activity, and showed little change in their kinetic parameters (Table 2). We therefore conclude that the quaternary structure is not required for catalytic activity, and moreover it appears that the formation of the dimer is not required to maintain stability towards inactivation by urea. The stability towards thermal inactivation was also very little affected. This is different from the situation in tetrameric aldolase from rabbit muscle where the disruption of the quaternary structure by mutagenesis resulted in catalytically active monomers at the expense of a substantial decrease in stability towards inactivation by both urea and temperature [17]. Previous work on homodimeric transaldolase from *Candida utilis* led to the proposal of half-of-the-sites reactivity for this enzyme [6]. Our finding that the monomeric mutants R300A and R300E show about the same level of activity as the dimeric wild-type enzyme does not support such a half-of-the-sites reactivity for the *E. coli* enzyme. Similar conclusions were put forward for transaldolase from *Saccharomyces cerevisiae* [18].

Acknowledgements: This work was supported by a grant from the Swedish Natural Science Research Council. U.S. and G.A.S. were supported by a grant of the Deutsche Forschungsgemeinschaft through SFB 380/Teilprojekt B21.

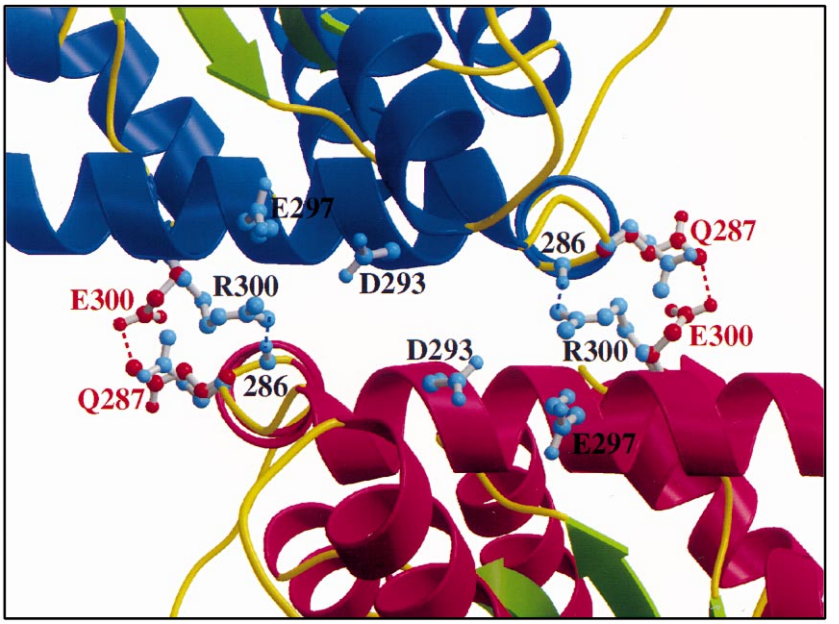

Fig. 2. Schematic view of the subunit-subunit interface of transaldolase. The two subunits are distinguished by different colors of the α-helices. Residues at the interface in the vicinity of the site of mutagenesis are included. Atoms color-coded blue represent side chain conformations of the wild-type enzyme, those colored red show the conformation in the R300E mutant. Hydrogen bonds (3.2 Å cutoff) are indicated by dashed lines. The picture was generated with MOLSCRIPT [19].

References

[1] Littlechild, J. and Watson, H.C. (1993) Trends Biol. Sci. 18, 36–39.
[2] Gefflaut, T., Blonski, C., Perie, J. and Willson, M. (1995) Prog. Biophys. Mol. Biol. 63, 301–340.
[3] Tsolas, O. and Horecker, B.L. (1972) in: The Enzymes, (Boyer, P.D., Ed.), Vol. 7, pp. 259–280, Academic Press, New York.
[4] Jia, J., Huang, W., Schörken, U., Sahm, H., Sprenger, G.A., Lindqvist, Y. and Schneider, G. (1996) Structure 4, 715–724.
[5] Lindqvist, Y. and Schneider, G. (1997) Curr. Opin. Struct. Biol. 7, 422–427.
[6] Grazi, E., Balboni, G., Brand, K. and Tsolas, O. (1977) Arch. Biochem. Biophys. 179, 131–135.
[7] Deng, W.P. and Nickoloff, J.A. (1992) Anal. Biochem. 200, 81–88.
[8] Sprenger, G.A., Schörken, U., Sprenger, G. and Sahm, H. (1995) J. Bacteriol. 177, 5930–5936.
[9] Bradford, M.M. (1976) Anal. Biochem. 72, 248–254.
[10] Jia, J., Lindqvist, Y., Schneider, G., Schörken, U., Sahm, H. and Sprenger, G.A. (1996) Acta Crystallogr. D 52, 192–193.
[11] Otwinowski, Z. (1993) Yale University Press, New Haven, CT.
[12] Jia, J. (1997) PhD thesis, Karolinska Institutet, Stockholm.
[13] Jones, T.A., Zou, J.Y., Cowan, S. and Kjeldgaard, M. (1991) Acta Crystallogr. A 47, 110–119.
[14] Brünger, A. (1989) Acta Crystallogr. A 45, 50–61.
[15] Engh, R.A. and Huber, R. (1991) Acta Crystallogr. A 47, 392–400.
[16] Laskowski, R.A., MacArthur, M.W., Moss, D.S. and Thornton, J.M. (1993) J. Appl. Crystallogr. 26, 946–950.
[17] Beernink, P.T. and Tolan, D.R. (1996) Proc. Natl. Acad. Sci. USA 93, 5374–5379.
[18] Miosga, T., Schaaff-Gerstenschläger, I., Franken, E. and Zimmermann, F.K. (1993) Yeast 9, 1241–1249.
[19] Kraulis, P. (1991) J. Appl. Crystallogr. 26, 282–291.